Friction velocity dependence of clay-rich fault material along a megasplay fault in the Nankai subduction zone at intermediate to high velocities

A. Tsutsumi, Olivier Fabbri, Anne Marie Karpoff, Kohtaro Ujiie, Atsushi Tsujimoto

Friction velocity dependence of clay-rich fault material along a megasplay fault in the Nankai subduction zone at intermediate to high velocities

Akito Tsutsumi,[1] Olivier Fabbri,[2] Anne Marie Karpoff,[3] Kohtaro Ujiie,[4] and Atsushi Tsujimoto[1]

Received 16 August 2011; revised 31 August 2011; accepted 1 September 2011; published 6 October 2011.

[1] The frictional properties of clay-rich fault material collected from a megasplay fault within the Nankai accretionary complex were examined in frictional experiments performed at a normal stress of 5 MPa under water-saturated conditions for slip velocities from 0.0026 to 260 mm/s with >250 mm of displacement. Our results reveal that the fault material can show two stages of velocity weakening behavior: weakening at slow velocities (v < 2.6 mm/s), characterized by a small degree of friction velocity dependence (the absolute value of ($a - b$) is typically <0.005), and a dramatic weakening at high velocities (v > 26 mm/s). Such a process of fault weakening may provide important constraints on models of faulting along a megasplay fault. At slip velocities from 0.026 to 2.6 mm/s, there exist both velocity-weakening and velocity-strengthening fault materials. The frictional coefficient values, μ, for slow slip velocities (v = 0.26 mm/s) are relatively low (μ = 0.28–0.35) for velocity-strengthening samples compared with velocity-weakening samples (μ = 0.38–0.49). Microstructural analyses reveal that velocity-strengthening samples show homogeneous deformation textures in which the entire gouge layer is deformed, whereas velocity-weakening materials show evidence of shear localization in which deformation is concentrated along narrow subsidiary shears.
Citation: Tsutsumi, A., O. Fabbri, A. M. Karpoff, K. Ujiie, and A. Tsujimoto (2011), Friction velocity dependence of clay-rich fault material along a megasplay fault in the Nankai subduction zone at intermediate to high velocities, *Geophys. Res. Lett.*, *38*, L19301, doi:10.1029/2011GL049314.

1. Introduction

[2] At the Nankai Trough margin, a large out-of-sequence fault system, termed the "megasplay fault," branches upward from the plate boundary to the seafloor, and has been implicated in coseismic slip and tsunami genesis [e.g., *Fukao*, 1979; *Park et al.*, 2002; *Moore et al.*, 2007]. An analysis of past frictional heating in materials along the megasplay fault in the Nankai accretionary prism has demonstrated that seismic fault slip propagated to the shallow up-dip end of the megasplay fault [*Sakaguchi et al.*, 2011]. Furthermore, recent seismological observations have revealed that very-low-frequency earthquakes (VLF) occur in the shallow portion of the Nankai Trough [*Ito and Obara*, 2006]. This finding suggests that earthquakes nucleate along the shallow parts of faults within the Nankai Trough. To understand the variety of earthquake phenomena in such a setting, it is important to study the frictional properties of shallow-level fault material within a subduction zone over a wide range of slip rates.

[3] In the context of rate- and state-dependent friction laws, the sliding behavior of a fault is governed by frictional velocity dependence $a - b$ and by the critical slip distance D_c [e.g., *Dieterich*, 1979, 1981; *Scholz*, 1998; *Marone*, 1998, and references therein]. The velocity dependence of clay-rich megasplay fault material along the megasplay fault, with the surrounding wall rocks, generally shows velocity strengthening at low slip rates (0.03-100 μm/s) [*Ikari et al.*, 2009a]. *Ujiie and Tsutsumi* [2010] reported high-velocity frictional data of the megasplay fault material, which are relevant to coseismic slip at velocities higher than 1 m/s. The authors showed that at high velocities, the frictional strength of the megasplay fault material becomes lower and D_c becomes larger than the values predicted by rate- and state-dependent friction laws. Consequently, the frictional constitutive parameters estimated for low slip rates (v < ~0.1 mm/s) may not be applicable to higher slip rates.

[4] Here, we present the results of a series of frictional experiments performed over a range of slip velocities from 0.0026 to 260 mm/s on the megasplay fault material from the Nankai accretionary complex. Knowledge of frictional properties at intermediate slip velocities should provide an important connection between the frictional behavior of seismic faults at slow and high slip rates.

2. Experimental Samples

[5] All of the samples tested in this study were collected from the Nankai accretionary prism, along a transect located offshore from Kii Peninsula, at Sites C0001 and C0004 during Integrated Ocean Drilling Program (IODP) Expedition 316 (Figure 1). At Site C0004, the drilling successfully penetrated the megasplay fault zone at 256–315 meters below the sea floor and collected fault zone materials (Figure 1) [*Expedition 316 Scientists*, 2009]. The fault zone consists of brecciated and fractured hemipelagic mudstone and volcanic ash layers [*Expedition 316 Scientists*, 2009]. Within the fault zone, a zone of slip localization is developed along a

[1]Department of Geology and Mineralogy, Division of Earth and Planetary Sciences, Graduate School of Science, Kyoto University, Kyoto, Japan.
[2]Geosciences, Université de Franche-Comté, Besançon, France.
[3]Institut de Physique du Globe de Strasbourg, CNRS, Université de Strasbourg, Strasbourg, France.
[4]Doctoral Program in Earth Evolution Sciences, Graduate School of Life and Environmental Sciences, University of Tsukuba, Tsukuba, Japan.

0094-8276/11/2011GL049314

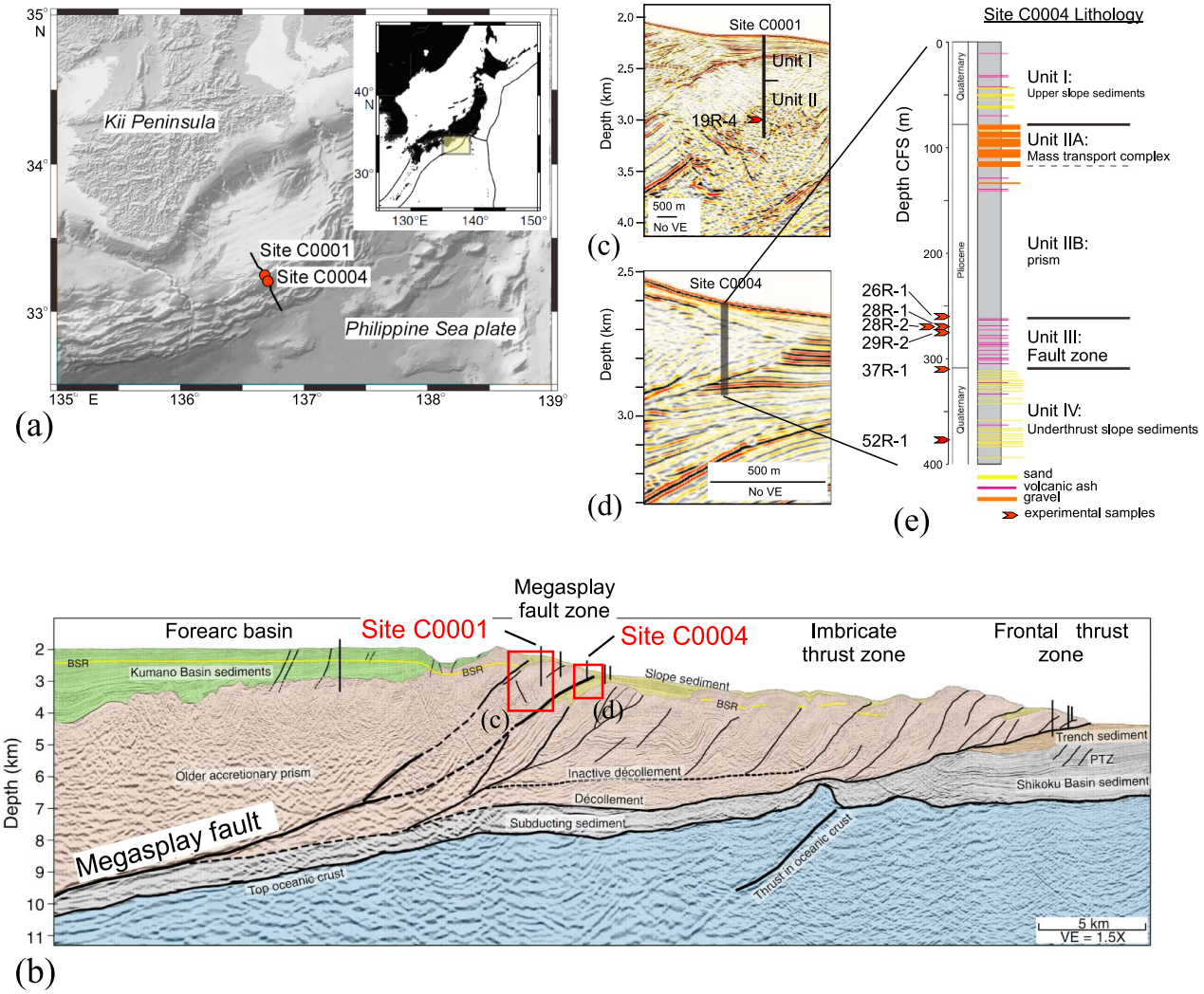

Figure 1. (a) Map of the Nankai area showing the location of drill sites C0004 and C0001, (modified from *Moore et al.* [2009]). (b) Interpreted cross-section showing the locations of drill sites C0004 and C0001 near the megasplay fault zone (modified from *Moore et al.* [2009]). Seismic profile (c) at site C0004 and (d) at site C0001 [after *Moore et al.*, 2007]. (e) Lithologic units at site C0004 (modified from *Expedition 316 Scientists* [2009]). Red arrows show the depth intervals of the core sections from which experimental samples were collected.

~10-mm-thick dark gouge in microbreccia [*Expedition 316 Scientists*, 2009]. Five fault rock samples and two host rock samples were used in the presented friction experiments, which were collected on board during Expedition 316. The fault rock samples include three fractured rocks, one fault breccia (C0004D-28R-2), and one microbreccia (C0004D-29R-2; see Table S1 in the auxiliary material for sample descriptions).[1] Among the fault rock samples, the fault breccia and the microbreccia were recovered from the fault core zone of the megasplay fault [*Expedition 316 Scientists*, 2009]; in fact, the fault breccia sample was collected from just 100 mm above the discrete zone of slip. One of the host rock samples was recovered from a core at Site C0001 (lithologic Unit II, upper accretionary prism of Pliocene age [*Expedition 315 Scientists*, 2009]), in the hanging wall of the mega-splay fault zone.

[6] Each of the sample core sections contains clay minerals (smectite, chlorite, illite and few kaolinite), quartz, plagioclase and calcite with total clay contents in a range from 53% to 64% [*Expedition 316 Scientists*, 2009; *Expedition 315 Scientists*, 2009]. A semi-quantitative X-ray diffraction (XRD) analysis of the oriented fine clay fractions from bulk samples revealed that the proportion of clay minerals is rather uniform with prevalent smectites, and the variations are subtle (see the auxiliary material for XRD data).

3. Experimental Procedure

[7] Friction experiments were conducted on the samples using a rotary-shear, intermediate- to high-velocity friction testing machine, as also used by *Ujiie and Tsutsumi* [2010]. The machine has a similar design to that of the machine used in previous high-velocity friction experiments [e.g., *Tsutsumi and Shimamoto*, 1997]. In addition to enabling high velocities (up to an equivalent velocity $v = 1.3$ m/s for a

[1]Auxiliary materials are available in the HTML. doi:10.1029/2011GL049314.

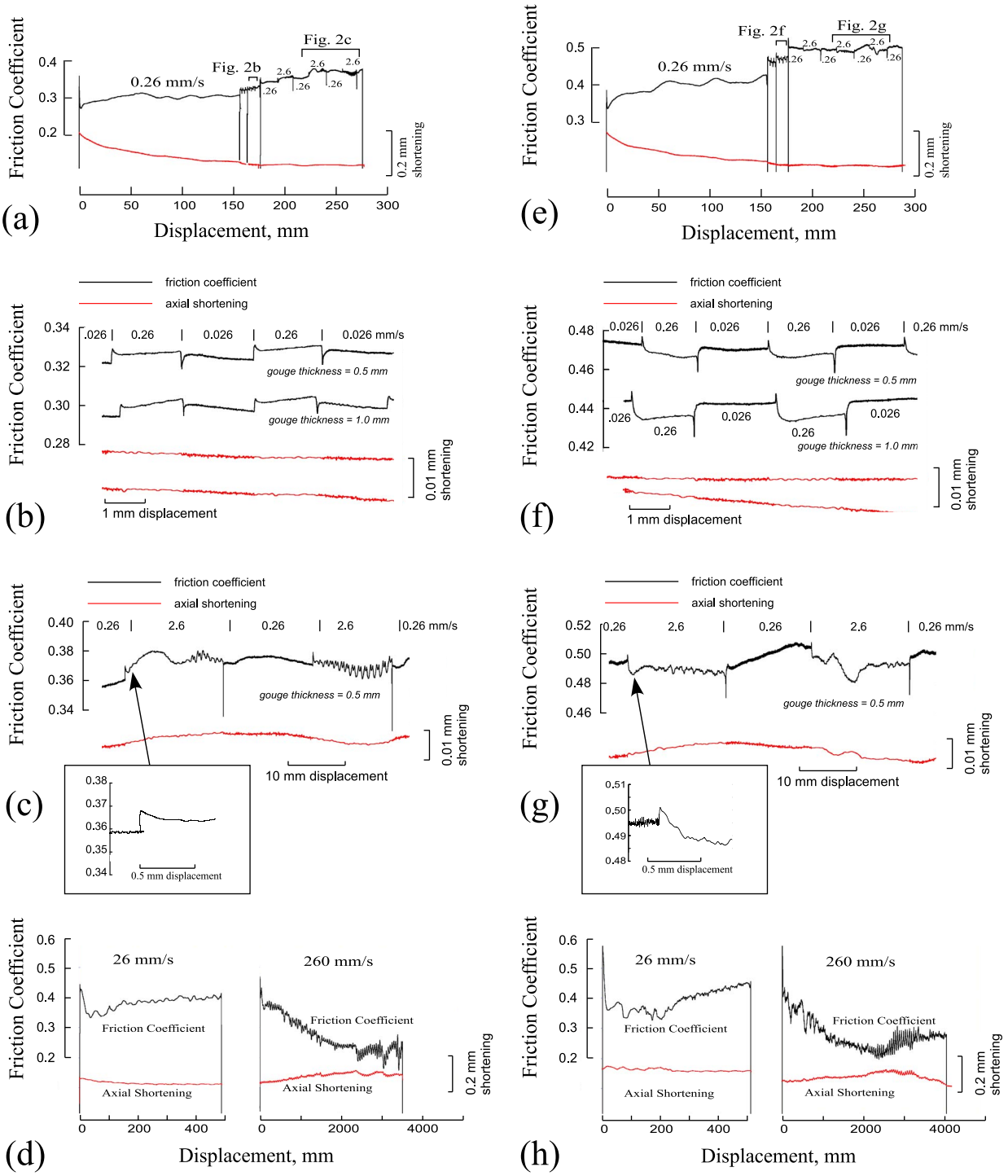

Figure 2. Evolution of the coefficient of friction and axial shortening of the gouge layer vs shear displacements for two representative fault samples, (a–d) C0004D-29R-2 and (e–h) C0004D-28R-2. A decrease in gouge-layer thickness is shown as a negative value. Velocity step tests employed velocities ranging from 0.026 to 2.6 mm/s. Note that sample C0004D-28R-2 shows a negative velocity dependence of friction and that C0004D-29R-2 shows a positive dependence. Constant velocity tests were performed at sliding velocities of 26 and 260 mm/s. Detailed views of the velocity steps are shown in Figures 2b and 2f for steps from 0.026 to 0.26 mm/s, and are shown in Figures 2c and 2g for steps from 0.26 to 2.6 mm/s. Inset figures show an enlarged plot at the time of the velocity step.

cylindrical sample of 25 mm in diameter), this apparatus is equipped with a servomotor and reduction gears to control the input rotation speed, enabling velocities as low as 0.0026 mm/s. The experimental fault consists of a pair of granite cylinders (25.0 mm in diameter) with an intervening thin layer of gouge (the initial gouge thickness was 0.5 mm except in the run denoted as "1.0 mm" in Figures 2b and 2f). A PTFE (Teflon) ring surrounds the fault to avoid gouge

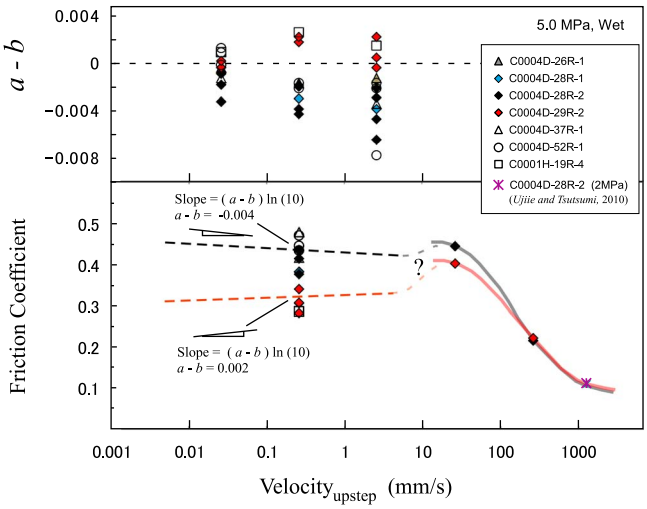

Figure 3. (top) Values of frictional velocity dependence, $a - b = \Delta\mu_{ss}/\Delta\ln V$ estimated from the velocity step curves in Figure 2 for a range of velocities (from 0.026 to 2.6 mm/s). Up-step velocities are used for the plot. (bottom) The velocity dependence of roughly steady state values of friction measured in constant velocity tests at a sliding velocity of 0.26 mm/s for all samples, and at 26 and 260 mm/s for the two representative samples, C0004D-28R-2 and C0004D-29R-2. Also shown for comparison are the results of high-velocity friction tests on a megasplay fault material at a sliding velocity of 1.3 m/s [from *Ujiie and Tsutsumi*, 2010]. Dashed lines indicate the approximate relationship between steady state friction values and slip velocities for low velocities, for the two representative fault rock samples, C0004D-29R-2 and C0004D-29R-2. Approximate steady state values of friction measured in constant velocity tests at $v = 0.26$ mm/s are used as reference points for drawing the dashed lines.

expulsion during rotation. The collected samples were disaggregated, oven dried at 50°C for 24 hours and then sieved to eliminate clasts larger than about 0.17 mm. Distilled water (0.5 ml) was added to the 0.5-mm-thick gouge layer (1.0 ml for the 1.0 mm gouge) to prepare saturated (wet) conditions for the experimental gouge layer. The assembled gouge was axially pre-compacted under the test conditions (5 MPa) for 30 min.

[8] All of the samples were subjected to an initial slip velocity of 0.26 mm/s until about 150 mm of displacement (three rotations of the sample cylinder), over which sliding the friction increased to attain a roughly steady state value and the gouge layer was compacted to about 0.1 mm in thickness (Figures 2a and 2e). After this pre-sliding, a sequence of velocity stepping by a factor of 10 was imposed for the velocity to examine the velocity dependence of friction, for loading velocities of 0.0026–2.6 mm/s and displacements of more than 250 mm (Figures 2a and 2e). Following the procedure described in previous studies [e.g., *Marone et al.*, 1990], we limited our measurement to the steady state portion of the friction curve after initial compaction (Figure 2).

[9] In addition to the velocity-step tests, constant-velocity tests were conducted for slip velocities of 26 and 260 mm/s to examine the way in which the steady-state level of friction changes with velocity at high velocities. An instantaneous velocity step-change test at high velocities, which would provide a direct measure of the velocity dependence, cannot be performed with our machine at the moment.

4. Experimental Results

[10] Velocity dependence was measured directly from plots of data like those in Figures 2b and 2f, as the frictional constitutive parameter combination $a - b$ ($= \Delta\mu_{ss}/\Delta\ln V$) for a step change in sliding velocity using the first several hundred microns of displacement after the up-step velocity changes.

[11] The samples tested in this study can be divided into two groups in regard to velocity dependence of steady state friction for velocities from 0.0026 to 2.6 mm/s (Figures 2 and 3). Samples of the first group, which is represented by sample C0004D-29R-2, show mainly neutral or positive velocity dependence, whereas those in the second group, which is represented by C0004D-28R-2, show negative velocity dependence. Two sets of representative results are shown in Figure 2. Note that the frictional behavior depends on the tested materials, and the results shown in Figures 2b and 2f are reproducible. Samples C0004D-29R-2 and C0004D-28R-2 showed consistently positive and negative velocity dependence, respectively, for initial gouge thicknesses of 0.5 and 1.0 mm. The friction value for the 1.0-mm-thick gouge is lower than for the 0.5-mm-thick layer (Figures 2b and 2f), possibly reflecting the difference in friction of the PTFE sleeves used in the experiments with different gouge thickness (the contact area between the granite cylinders and the internal surface of the PTFE sleeve is smaller for the 1.0-mm-thick gouge samples). Further work is needed to evaluate the effect on friction of the PTFE sleeve.

[12] Steady state friction values for lower velocities ($v <$ 26 mm/s) are difficult to measure because the friction value fluctuates with slip. Note that the friction at $v = 0.26$ mm/s fluctuates with a long wavelength (~50 mm of displacement), most likely reflecting the rotation of the sample (Figures 2a and 2e). For sliding at $v = 2.6$ mm/s, the friction fluctuates at a higher frequency (Figures 2c and 2g), for which the average wavelength is 1–2 mm of displacement. The cause of this behavior remains unknown. The amplitude of these fluctuations is sometimes larger than the measured values of the instantaneous friction velocity dependence.

[13] The frictional coefficient determined at a velocity of 26 mm/s initially decreases from 0.42 to 0.33 (e.g., sample C0004D-29R-2) and then increases gradually to attain a roughly constant friction value of about 0.4 (Figure 2d). At a velocity of 260 mm/s, the friction coefficient shows a gradual decrease with a large weakening displacement toward the establishment of a nearly constant level of friction at 0.2–0.25 (Figure 2d). Thus a dramatic slip weakening with large weakening displacement (>~2000 mm) characterizes the frictional behavior of the sample slid at 260 mm/s (Figure 2).

5. Deformation Textures

[14] Microstructural observations of the deformation textures generated during the friction experiments reveal that velocity-strengthening samples possess a homogeneous deformation texture in which the entire gouge layer is deformed, whereas, the velocity-weakening samples contain

a shear localization texture in which deformation is concentrated along narrow subsidiary shears (see auxiliary material).

6. Discussion and Conclusions

[15] The results reveal that fault rocks in megasplay fault zones within the shallow portion of the Nankai accretionary prism can exhibit not only a positive velocity dependence of friction but also a negative velocity dependence under wet conditions for a range of sliding velocities from 0.026 to 2.6 mm/s at large shear displacements of more than 150 mm. It could be argued that this result appears to be inconsistent with a previous study that reported completely positive dependence of friction in the case of clay-rich megasplay fault material [*Ikari et al.*, 2009a]. We interpret that the negative velocity dependence is due to the development of localized shear textures (see auxiliary material) at large shear displacements. The higher than previously studied range of sliding velocities of our study may also be an important factor for the textural development. As reported in many references, a large shear displacement induces structural evolution in a gouge shear zone from distributed shearing to slip localization along Y-shears and the localization is associated with a change from velocity-strengthening to velocity-weakening frictional behavior [e.g., *Dieterich*, 1981; *Moore et al.*, 1989; *Logan et al.*, 1992; *Beeler et al.*, 1996; *Ikari et al.*, 2011]. The negative velocity dependence of friction observed in the present study for experimental gouge may represent a corresponding transition from distributed to localized shear during the initial sliding to a displacement of 150 mm. In fact, with ongoing displacement, some of the samples showed a transition from a slightly positive velocity dependence to a negative dependence within the slowest range of slip velocities from 0.0026 to 0.026 m/s (Figure 3).

[16] The present results suggest that shear localization at intermediate velocities plays an important role in controlling the velocity dependence of friction for megasplay fault materials. Nevertheless, it should be noted that not all the tested gouge materials exhibited a negative velocity dependence (Figure 3). What properties control whether the steady-state deformation textures within gouge samples become pervasive or localized?

[17] Although the available data are still limited, our experimental results show that the friction values of the velocity-strengthening samples are relatively low compared with those of the velocity-weakening samples (Figures 2 and 3). Similar relationships between frictional strength and the velocity dependence of clayey gouges have been reported by *Ikari et al.* [2011] for experiments performed in a range of slip velocities from 0.001 to 0.3 mm/s. Low values of friction may indicate a higher content of weak clays in gouge layers [e.g., *Summers and Byerlee*, 1977; *Morrow et al.*, 1992, 2000; *Brown et al.*, 2003: *Kopf and Brown*, 2003; *Moore and Lockner*, 2004; *Ikari et al.*, 2009a, 2009b; *Tembe et al.*, 2010]. However, variation of the total amount of clays within the tested samples of our study must be small, within a range from ~53–64% [*Expedition 316 Scientist*, 2009; *Expedition 315 Scientist*, 2009]. For example, sample section interval for C0004D-28R-2 contains ~53% of total clays, and sample section C0004D-29R-2 contains ~61% clays (see auxiliary material), thus the difference is <10% [*Expedition 316 Scientists*, 2009]. In addition, as noted above, clay composition is more or less uniform and the variations are subtle (see auxiliary material). This observation would imply that the different deformation textures were not influenced by the clay content or by the composition of clays in the samples.

[18] It is not clear what material properties control the development of deformation textures and the frictional velocity dependence. However, the observed relations among frictional strength, the velocity dependence of friction, and deformation texture have important implications for earthquake mechanics along megasplay faults. It is suggested that localized shear deformation, which is characteristic of a velocity-weakening fault, could occur along a section of fault with high frictional strength, whereas, deformation may be distributed along a section of the fault that is relatively weak, corresponding to a positive frictional velocity dependence.

[19] Our results reveal that clay-rich megasplay fault materials from the Nankai accretionary prism show two stages of velocity weakening behavior; weakening for a range of slow velocities ($v < 2.6$ mm/s), which is characterized by a small degree of the friction velocity dependence (the absolute value of $(a - b)$ is typically <0.005, Figure 3), and a dramatic weakening at high velocities ($v > 26$ mm/s) (Figure 3). Such a process of fault weakening may provide important constraints on models of faulting along a megasplay fault. Velocity weakening behavior would contribute to initiate unstable fault motion along a fault at shallow depths; e.g., VLF events within the shallow portion of the Nankai accretionary prism [*Ito and Obara*, 2006]. The frictional strength of a fault would show a marked decrease with further increases in slip amount and slip rate, if the amount of fault slip is sufficiently large compared with the large weakening distance D_c observed for high-velocity weakening (Figures 2d and 2h). Such a weakening process would cause fault instability that fosters seismic slip along a megasplay fault at shallow depths. In contrast, velocity strengthening behavior at slow to intermediate velocities may act to stabilize the propagation of earthquake ruptures that nucleate in the velocity weakening portion of a fault [e.g., *Scholz*, 1998].

[20] **Acknowledgments.** This research used samples and data provided by the Integrated Ocean Drilling Program (IODP). The authors gratefully acknowledge the support provided by the operation staff of D/V *Chikyu* and the onboard laboratory technicians (Marine Works Japan). We thank H. Kitajima and an anonymous reviewer for their constructive comments and suggestions, which led to improvements in the paper. This research was supported by MEXT Japan, under its Observation and Research Program for Prediction of Earthquakes and Volcanic Eruptions project, and by MEXT KAKENHI 21107004.

References

Beeler, N. M., T. E. Tullis, M. L. Blanpied, and J. D. Weeks (1996), Frictional behavior of large displacement experimental faults, *J. Geophys. Res.*, *101*, 8697–8715, doi:10.1029/96JB00411.

Brown, K. M., A. Kopf, M. B. Underwood, and J. L. Weinberger (2003), Compositional and fluid pressure controls on the state of stress on the Nankai subduction thrust: A weak plate boundary, *Earth Planet. Sci. Lett.*, *214*, 589–603, doi:10.1016/S0012-821X(03)00388-1.

Dieterich, J. H. (1979), Modeling of rock friction 1. Experimental results and constitutive equations, *J. Geophys. Res.*, *84*, 2161–2168, doi:10.1029/JB084iB05p02161.

Dieterich, J. H. (1981), Constitutive properties of faults with simulated gouge, in *Mechanical Behavior of Crustal Rocks: The Handin Volume*, *Geophys. Monogr. Ser.*, vol. 24, edited by N. L. Carter et al., pp. 103–120, AGU, Washington, D. C.

Expedition 315 Scientists (2009), Expedition 315 Site C0001, in *NanTroSEIZE Stage 1: Investigations of Seismogenesis, Nankai Trough,*

Japan, *Proc. Integr. Ocean Drill. Program*, *314/315/316*, doi:10.2204/iodp.proc.314315316.123.2009.

Expedition 316 Scientists (2009), Expedition 316 Site C0004, in *NanTroSEIZE Stage 1: Investigations of Seismogenesis, Nankai Trough, Japan*, *Proc. Integr. Ocean Drill. Program*, *314/315/316*, doi:10.2204/iodp.proc.314315316.133.2009.

Fukao, Y. (1979), Tsunami earthquakes and subduction processes near deep-sea trenches, *J. Geophys. Res.*, *84*, 2303–2314, doi:10.1029/JB084iB05p02303.

Ikari, M. J., D. M. Saffer, and C. Marone (2009a), Frictional and hydrologic properties of a major splay fault system, Nankai subduction zone, *Geophys. Res. Lett.*, *36*, L20313, doi:10.1029/2009GL040009.

Ikari, M. J., D. M. Saffer, and C. Marone (2009b), Frictional and hydrologic properties of clay-rich fault gouge, *J. Geophys. Res.*, *114*, B05409, doi:10.1029/2008JB006089.

Ikari, M. J., C. Marone, and D. M. Saffer (2011), On the relation between fault strength and frictional stability, *Geology*, *39*, 83–86, doi:10.1130/G31416.1.

Ito, Y., and K. Obara (2006), Dynamic deformation of the accretionary prism excites very low frequency earthquakes, *Geophys. Res. Lett.*, *33*, L02311, doi:10.1029/2005GL025270.

Kopf, A., and K. M. Brown (2003), Friction experiments on saturated sediments and their implications for the stress of the Nankai and Barbados subduction thrusts, *Mar. Geol.*, *202*, 193–210, doi:10.1016/S0025-3227(03)00286-X.

Logan, J. M., C. A. Dengo, N. G. Higgs, and Z. Z. Wang (1992), Fabrics of experimental fault zones: Their development and relationship to mechanical behavior, in *Fault Mechanics and Transport Properties of Rocks*, edited by B. Evans and T. F. Wong, pp. 33–67, Academic, San Diego, Calif., doi:10.1016/S0074-6142(08)62814-4.

Marone, C. (1998), Laboratory-derived friction laws and their application to seismic faulting, *Annu. Rev. Earth Planet. Sci.*, *26*, 643–696, doi:10.1146/annurev.earth.26.1.643.

Marone, C., C. B. Raleigh, and C. H. Scholz (1990), Frictional behavior and constitutive modeling of simulated fault gouge, *J. Geophys. Res.*, *95*, 7007–7025, doi:10.1029/JB095iB05p07007.

Moore, D. E., and D. A. Lockner (2004), Crystallographic controls on the frictional behavior of dry and water-saturated sheet structure minerals, *J. Geophys. Res.*, *109*, B03401, doi:10.1029/2003JB002582.

Moore, D. E., R. Summers, and J. D. Byerlee (1989), Sliding behavior and deformation textures of heated illite gouge, *J. Struct. Geol.*, *11*, 329–342, doi:10.1016/0191-8141(89)90072-2.

Moore, G. F., N. L. Bangs, A. Taira, S. Kuramoto, E. Pangborn, and H. J. Tobin (2007), Three-dimensional splay fault geometry and implication for Tsunami generation, *Science*, *318*, 1128–1131, doi:10.1126/science.1147195.

Moore, G. F., et al. (2009), Structural and seismic stratigraphic framework of the NanTroSEIZE Stage 1 transect, in *NanTroSEIZE Stage 1: Investigations of Seismogenesis, Nankai Trough, Japan*, *Proc. Integr. Ocean Drill. Program*, *314/315/316*, doi:10.2204/iodp.proc.314315316.102.2009.

Morrow, C., B. Radney, and J. Byerlee (1992), Frictional strength and effective pressure law of montmorillonite and illite clays, in *Fault Mechanics and Transport Properties of Rocks*, edited by B. Evans and T. F. Wong, pp. 69–88, Academic, San Diego, Calif., doi:10.1016/S0074-6142(08)62815-6.

Morrow, C. A., D. E. Moore, and D. A. Lockner (2000), The effect of mineral bond strength and adsorbed water on fault gouge frictional strength, *Geophys. Res. Lett.*, *27*, 815–818, doi:10.1029/1999GL008401.

Park, J.-O., T. Tsuru, S. Kodaira, P. R. Cummins, and Y. Kaneda (2002), Splay fault branching along the Nankai subduction zone, *Science*, *297*, 1157–1160, doi:10.1126/science.1074111.

Sakaguchi, A., et al. (2011), Seismic slip propagation to the updip end of plate boundary subduction interface faults: Vitrinite reflectance geothermometry on Integrated Ocean Drilling Program NanTroSEIZE cores, *Geology*, *39*, 395–398, doi:10.1130/G31642.1.

Scholz, C. H. (1998), Earthquakes and friction laws, *Nature*, *391*, 37–42, doi:10.1038/34097.

Summers, R., and J. Byerlee (1977), A note on the effect of fault gouge composition on the stability of frictional sliding, *Int. J. Rock Mech. Min. Sci.*, *14*, 155–160, doi:10.1016/0148-9062(77)90007-9.

Tembe, S., D. A. Lockner, and T.-F. Wong (2010), Effect of clay content and mineralogy on frictional sliding behavior of simulated gouges: Binary and ternary mixtures of quartz, illite, and montmorillonite, *J. Geophys. Res.*, *115*, B03416, doi:10.1029/2009JB006383.

Tsutsumi, A., and T. Shimamoto (1997), High-velocity frictional properties of gabbro, *Geophys. Res. Lett.*, *24*, 699–702, doi:10.1029/97GL00503.

Ujiie, K., and A. Tsutsumi (2010), High-velocity frictional properties of clay-rich fault gouge in a megasplay fault zone, Nankai subduction zone, *Geophys. Res. Lett.*, L24310, doi:10.1029/2010GL046002.

O. Fabbri, Geosciences, Université de Franche-Comté, 16 route de Gray, F-25030 Besançon CEDEX, France.

A. M. Karpoff, Institut de Physique du Globe de Strasbourg, CNRS, Université de Strasbourg, F-67084 Strasbourg CEDEX, France.

A. Tsujimoto and A. Tsutsumi, Department of Geology and Mineralogy, Division of Earth and Planetary Sciences, Graduate School of Science, Kyoto University, Kita-shirakawa, Sakyo-ku, Kyoto 606-8502, Japan. (tsutsumi@kueps.kyoto-u.ac.jp)

K. Ujiie, Doctoral Program in Earth Evolution Sciences, Graduate School of Life and Environmental Sciences, University of Tsukuba, 1-1-1 Tennodai, Tsukuba, Ibaraki 305-0006, Japan.